15C.7 INTENSITY, STRUCTURE AND RAINFALL IN HIGH-RESOLUTION NUMERICAL SIMULATIONS OF TYPHOON MORAKOT (2009)

Jonathan Hall[1,2,*], Ming Xue[1], Lance Leslie[2], Kun Zhao[1], Linkun Ran[1] and Fanyou Kong[1]

[1]Center for Analysis and Prediction of Storms and [2]School of Meteorology
University of Oklahoma, Norman Oklahoma

1. INTRODUCTION

Typhoon Morakot claimed a heavy toll in terms of lives lost and material damages over the northwest Pacific in August 2009. The impact on the island of Taiwan was particularly devastating, with estimates of around 700 lives lost and some NT$110 billion (US$3.3 billion) in damages, mainly due to flooding, landslides and debris flows. Although Morakot was only a moderate intensity typhoon at landfall, it was a large and relatively slow-moving storm, and it produced extreme rainfall over southern parts of Taiwan, reaching 1404 mm in 24 hours at Weiliao Mountain in Pingtung County, and a three day storm total of 2884 mm at Alishan, both of which are records for Taiwan and relatively close to world record values (these locations are indicated in Fig. 1).

Typhoon Morakot developed near the centre of a large monsoon gyre circulation about 1300 km east of Taiwan in early August 2009, and adopted an almost due westerly track towards the island. To the west, a very moist monsoon southwesterly flow regime was in place over the southern South China Sea, and this was being enhanced by the presence of another tropical cyclone (TC), Tropical Storm Goni, which was near stationary over the island of Hainan. As Morakot approached Taiwan on the 7th and 8th, a surge in the monsoon flow advected this deep, moist airmass northeastwards towards the island, with precipitable water values reaching 70 to 75 mm as the landfall phase occurred, well above the long term mean for August over the area of about 45 to 50 mm.

Morakot peaked in intensity with sustained winds of about 40 ms^{-1} while still well off the east coast of Taiwan. As the cyclone began to approach the coast, dryer mid-level air began to wrap into the circulation from the north, and this combined with moderate vertical wind shear halted its strengthening and led to the deep convection taking on an asymmetric structure, becoming increasingly confined to the southern semi-circle as landfall was approached. In part, this slight increase in vertical wind shear was due to the increasing low level monsoon flow, and this also provided a gradually increasing southerly steering influence over the system.

Overland rainfall patterns and intensities produced by TCs are sensitive to the details of the track, and changing structure of the TC during landfall. In the case of Taiwan, both of these aspects are significantly affected by the high terrain of the Central Mountain Range (CMR), which is oriented NNE to SSW along the spine of the island (Fig. 1). Previous observational and modeling studies have investigated track changes in landfalling typhoons as they interact with the CMR. Wang (1980), in an observational study, showed that the results of this interaction produced two basic types of track in the impacting TC; either the track was continuous, with various amounts of cyclonic deflection, or discontinuous, with the original low-level centre dissipating on the windward side of the island whilst a new centre develops on the lee side beneath the westward tracking mid-level centre. Subsequent observational and modeling studies have generally confirmed and reinforced these observations, and shown that the track type is quite sensitive to the size, intensity and forward speed of the TC (Lin et. al. 2005). This latter study showed that features of the TC favoring the discontinuous track type were a relatively large size, slow forward speed and weak to moderate intensity; stronger, faster-moving and smaller systems tended to display a continuous track across the island.

Although Taiwan regularly experiences the impact of typhoons (on average about 1.8 per year affect the island, Zhang et. al. 2009) and resultant flooding, the Morakot case was of unprecedented intensity in modern times. This naturally raises the questions: what made this system unusual amongst other landfalling TCs? Will it be possible to forecast the next similar event? The first step in the direction towards

* *Corresponding author address:* Jonathan Hall, University of Oklahoma, School of Meteorology, 120 David L Boren Blvd., Norman Oklahoma 73072.

answering these questions is to accurately reproduce the Morakot case in high resolution models.

2. DATA AND MODELS

2.1 *Numerical Models*

A series of simulations of Morakot were undertaken utilizing version 5.2 of the Advanced Regional Prediction System (ARPS) developed at the Center for Analysis and Prediction of Storms (Xue et. al., 2003), a cloud resolving, non-hydrostatic mesoscale model with a terrain following vertical coordinate.

All model runs used the operational analyses of the 0.5 degree Global Forecast System (GFS) global model for initial conditions. Due to the relatively large scale of the monsoon gyre and circulation of Morakot, the GFS resolved the system well, and hence spin-up time for the ARPS runs appeared to be minimal. Boundary conditions during each run were also obtained from the GFS analyses. ARPS was run one-way nested on 15 km and 3 km stationary grids with 53 vertical levels. The 15 km domain covered an area of 9045 km by 6045 km centered at 28N 125E, while the 3 km grid spanned 3009 km by 2409 km. Vertical levels were stretched to give more resolution in the boundary layer and near the tropopause. The physics packages for all the ARPS runs included 1.5 order turbulence closure with the Sun and Chang PBL scheme; the 15 km runs incorporated the Kain and Fritsch convective parameterization, while the 3 km nested runs were cloud resolving using the Lin microphysics scheme. Initial experiments have consisted of individual 15 km runs initialized every 6 hours commencing 1200UTC 5 August until 0000UTC 8 August (all subsequent references to time will be in UTC), and 3 km runs initialized at 3 hourly intervals between 0000 7 August to 0600 8 August inclusive. All of these experiments were undertaken incorporating realistic terrain, with a 30 arc second resolution (or approximately 900 metres).

3. RESULTS

3.1 *Observations*

An observational analysis of the Morakot case indicates that it displayed the discontinuous track type during its passage across Taiwan, in keeping with its relatively large size, slow motion and moderate intensity, with estimated maximum sustained winds on approach to landfall of about 40 m s^{-1} . This can clearly be seen in the composite reflectivity field from the Taiwan radar mosaic displayed in Fig. 2. Satellite imagery and surface observations also depict the initial low level centre being deflected northwards towards the northern tip of the island and weakening, whilst a new low level circulation develops over central the western Taiwan lowlands by about 0000 8 August. At the same time, deep convection associated with the mid-level vortex could be tracked westwards across the island, although weakening with time. The principle rainband remained almost stationary near the southern tip of the island during the landfall phase, although satellite imagery indicates that convection within this band was relatively weak and low-topped. For a short period of time from 0000 on the 8th, the centre of the typhoon was virtually devoid of deep convection, until about 0600 when fresh convective blooms developed in a secondary band around the southern flank of the new low level centre, as it drifted west into the Taiwan Strait. This band eventually consolidated and developed eastwards into the CMR, where it was enhanced and sustained by the upslope flow on the western side of the mountains. The new centre was initially slow-moving off the west coast of Taiwan, before adopting a slow north-northwest track towards the coast of China, crossing the coast near Nangang at 1200 9 August.

It should be noted that the complex nature of the track of Morakot near Taiwan made production of the official best track by the responsible agencies quite difficult. This can be seen in the variation in best tracks produced by the Joint Typhoon Warning Center (JTWC), Japan Meteorological Agency (JMA) and the China Meteorological Administration (CMA), in which the centre location differed by as much as 160 km as the typhoon crossed Taiwan. For this reason, emphasis is placed upon the observations when verifying the individual model runs, rather than relating to any of the best tracks.

3.2 *Model results*

In the following discussion, model runs will be referred to by their initialization time in the format ddhh, where dd is the day and hh is the hour in UTC. Generally, all model runs captured the evolving asymmetric structure of Morakot as the effects of northerly vertical shear and dryer air intrusion led to deep convection becoming confined to the southern side. The near-stationary principle rainband lying east/west near the southern tip of Taiwan during the landfall phase was also well represented.

Figure 3 shows a time series of the intensity, represented by maximum sustained winds, for the 0712 runs compared to the best track estimates from the three agencies. Virtually all runs displayed a slight

weakening for the first six hours, with a leveling off in intensity for those members with the typhoon still over the ocean from then until landfall. A very slight re-intensification can be seen in the 3 km run as the new centre moves over the waters of the Taiwan Strait, before the systems weaken once more as it moves north.

In terms of the tracks, the main contrast between the 15 km and 3 km ARPS runs was in the movement of the low level centre across the CMR. As will be seen, this is crucial to the ultimate impact of the modeled typhoon on Taiwan in terms of rainfall. All of the 15 km runs produced a continuous track type, with the TC moving on a cyclonic curve about the north of the island, and then moving off to the north-northwest – the track of the 0700 run displayed in Fig. 4a is representative of this behavior. Primarily for this reason, the simulated total rainfall over southern Taiwan for all the 15 km runs was significantly too low, with peaks in the CMR of around 750 mm – Fig 5a displays the total rainfall for the 0700 run, and other runs produced similar results. With no development of a secondary low level centre to the west of the island, there is a lack of a focus for convergence with the southwesterly monsoon flow, and hence the banding of deep convection seen in the observations did not occur. Since the track is so different, it is difficult to estimate other effects, such as the coarser resolution or parameterized cumulus convection. Operational runs of the GFS 0.5 degree model displayed very similar behavior to the ARPS 15 km runs (not shown), featuring the continuous, cyclonically curved track type across northern Taiwan.

As seen in Fig 4c, runs at 3 km resolution initialized before 0600 7 August displayed similar behavior, although the tracks were consistently to the left of the 15 km runs, and passed over northern Taiwan. The 3 km runs commenced from 0600 7 August and later displayed the discontinuous track type across the island with a new centre developing to the west of the CMR, and therefore matched the observations much more closely, as will be seen below. The reasons for the difference in track types between the 15 km and later 3 km runs are difficult to quantify and are a subject of ongoing investigation. One factor may be differences in vertical coupling between the parameterized and explicitly resolved convection, with the 15 km runs responding more readily to the increasing low level steering flow.

The formation of the new low level centre in the later 3 km runs led to the development of a persistent convergence band with the strengthening monsoon flow on its southern flank, and a band of heavy convective rainfall developing into the central southern CMR. This effect is displayed in Fig. 6, emphasizing the contrast between the early and late 3 km runs, and resultant structure of deep convection over southern Taiwan. It is also clear from Fig 6 that the 0712 run is far more consistent with the radar and surface observations than the 0700 run, something that is even more clear in animations.

Storm total rainfall from the 0712 run for the 36 hours from initialization until 0000 9 August is displayed in Fig 5b. All of the 3 km runs with discontinuous tracks produced similar rainfall patterns and amounts to those seen here, with peaks totals typically on the order of 1800 mm along the southern parts of the CMR. It is clear from Fig 5c that this result matches very well with the observations over these southern parts of the island.

Further north in the Alishan area, where the highest totals for the event were recorded, the models did produce heavy rainfall, but failed to capture the peak. Close inspection of the animated radar mosaic indicates that the initial secondary convergence banding moved slowly south and merged with the principle rainband of the TC, while a new secondary band developed in its place and eventually affected the Alishan area. The model runs did reproduce some evidence of this secondary development, but due to the new surface centre moving to the north slightly too quickly, this band was displaced slightly to the north and west and did not affect the Alishan area. The reasons for the model ejecting the surface low slightly too rapidly remain as a feature to be investigated.

REFERENCES

Lin, Y.-L., S.-Y. Chen, and C. M. Hill, 2005: Control parameters for the influence of a mesoscale mountain range on cyclone track continuity and deflection. *J. Atmos. Sci.,* **62,** 1849-1866.

Wang, S.-T., 1980: Prediction of the behavior and strength of typhoons in Taiwan and its vicinity. Research Report 108, Chinese National Science Council, Taipei, Taiwan. 100 pp. (In Chinese)

Xue, M., D.-H. Wang, J.-D. Gao, K. Brewster, and K. K. Droegemeier, 2003: The Advanced Regional Prediction System (ARPS), storm-scale numerical weather prediction and data assimilation. *Meteor. Atmos. Physics*, **82,** 139-170.

Zhang, Q., L. Wu, and Q. Liu, 2009: Tropical cyclone damages in China. *Bull. American Met. Soc.,* **90,** 489-495.

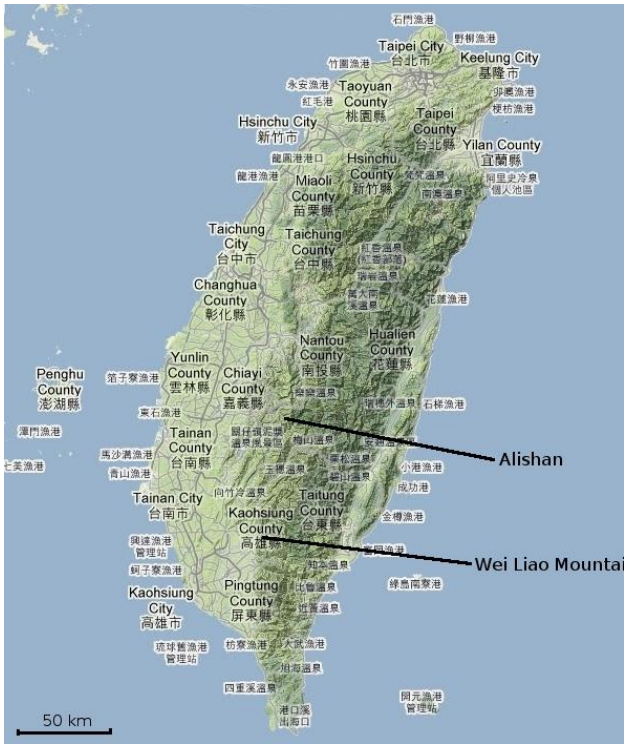

Figure 1. Map of Taiwan, showing the locations observing extreme rainfall mentioned in the text.

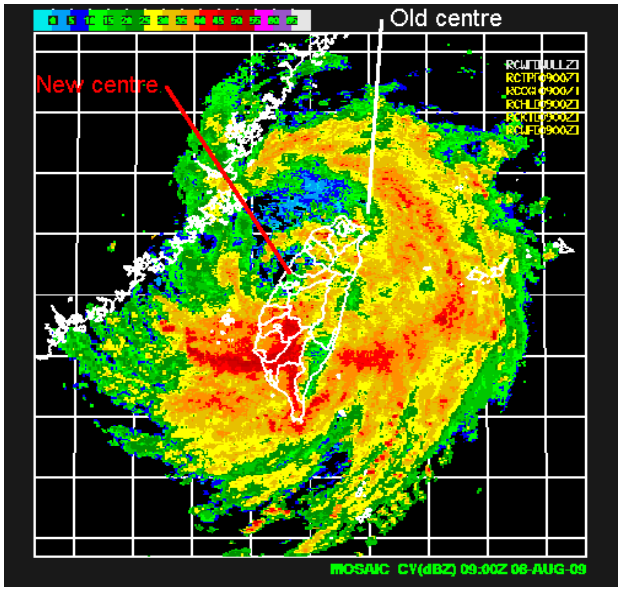

Figure 2. Composite reflectivity from merged radar imagery over Taiwan at 0000UTC 8 August 2009. Locations of the original (old) surface centre and the newly developing surface centre are indicated.

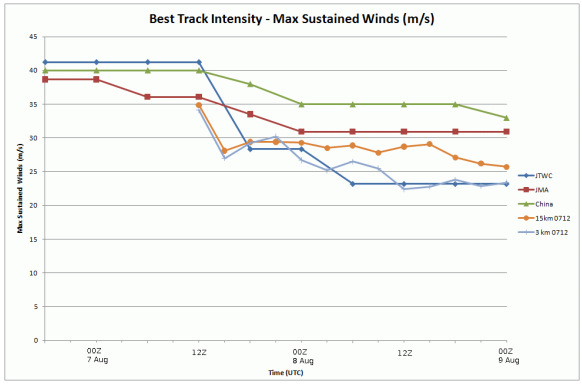

Figure 3. Intensity time series, measured by maximum sustained winds, from official best tracks from JTWC, JMA and CMA, along with model results from the 0712 runs at 15 km and 3 km.

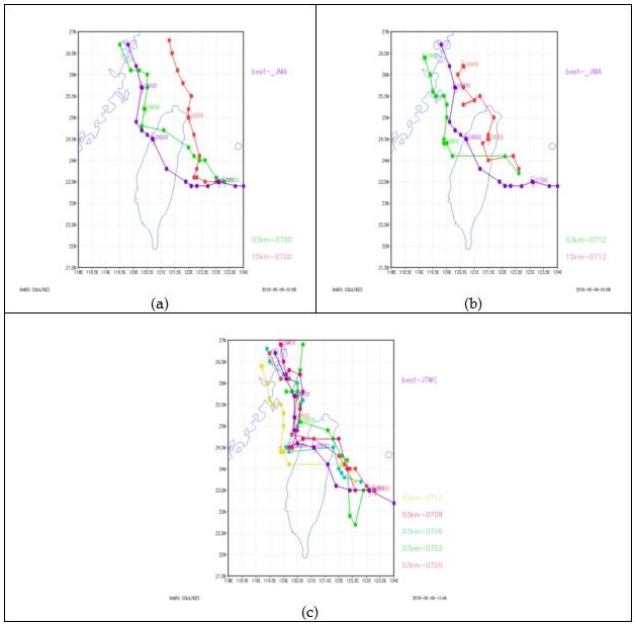

Figure 4. Tracks of various model runs, with JTWC best track, (a) 0700 runs at 15 km and 3 km; (b) same as (a) except for 0712 runs; (c) 3 km runs initialized between 0700 and 0712.

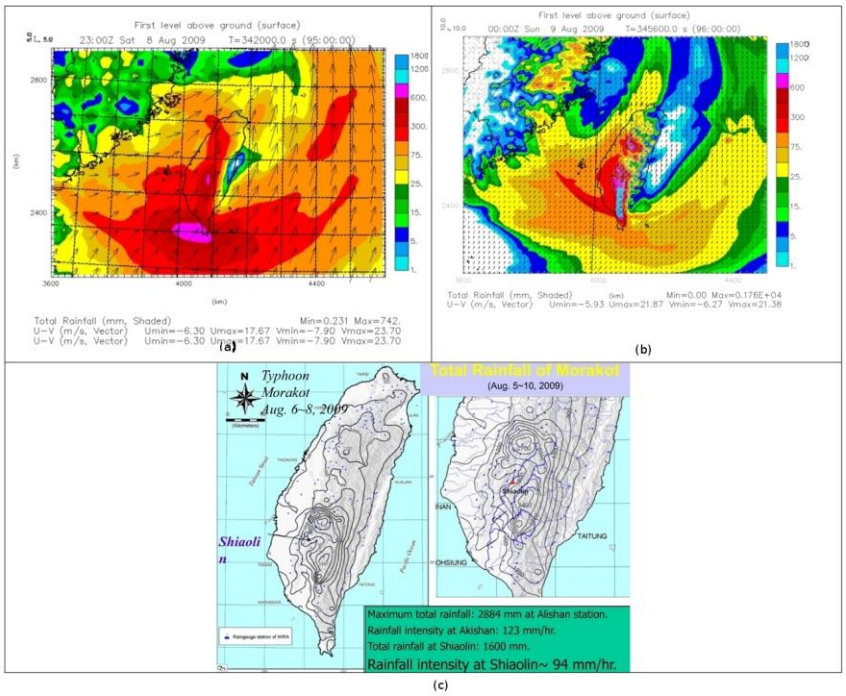

Figure 5. Total accumulated rainfall from (a) 0700 15 km run, and (b) 0712 3 km run, compared with (c) storm totals estimated from rain guage analyses

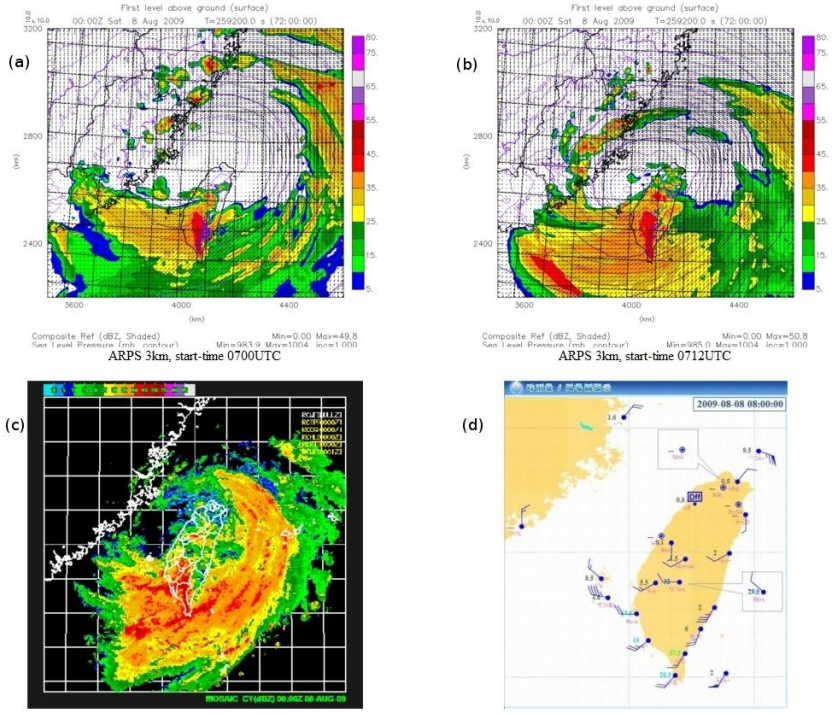

Figure 6. Comparison of 0700 and 0712 runs verifying at 0000UTC 8 August. (a) and (b) show composite reflectivity and surface winds from the 0700 and 0712 runs respectively, (c) radar mosaic of composite reflectivity with identical color scale. (d) Surface observations, indicating winds and hourly rainfall. Note in (d) wind speeds are in knots, and time is labeled in local time, and is equivalent to 0000UTC.